Classical and Quantum Gravity

PAPER

Tetrahedral omnidirectional full-tensor gravitational wave detector

To cite this article: Zachary Metzler *et al* 2022 *Class. Quantum Grav.* **39** 225012

IOP Publishing Classical and Quantum Gravity
Class. Quantum Grav. **39** (2022) 225012 (9pp) https://doi.org/10.1088/1361-6382/ac902d

Tetrahedral omnidirectional full-tensor gravitational wave detector

Zachary Metzler, Christopher J Collins, Ho Jung Paik* and Peter S Shawhan

Department of Physics, University of Maryland, College Park, MD 20742, United States of America

E-mail: hpaik@umd.edu

Received 10 May 2022, revised 27 July 2022
Accepted for publication 7 September 2022
Published 24 October 2022

Abstract

We propose a new tetrahedral configuration of three-axis inertial sensors, whose signals when combined create an isotropic sensitivity to gravitational waves. This arrangement provides total sky coverage and full-tensor measurements of the gravity gradient using only four test masses (TMs), compared to the six TMs of the previously studied TIGA and superconducting omnidirectional gravitational radiation observatory designs. Since weakly suspending a TM in all three directions is difficult due to the gravity bias, we also present the directional sensitivity plot for the case where only horizontal displacements are measured. This antenna pattern is no longer isotropic, and results in a maximum sensitivity to minimum sensitivity ratio of 2:1 in power. The full gravity gradient tensor can in this case still be reconstructed if the platform is sufficiently isolated from ground tilt.

Keywords: gravitational wave detection, tensor gravitational wave detector, tetrahedral configuration

(Some figures may appear in colour only in the online journal)

1. Background

A longstanding goal for gravitational wave (GW) detection has been the development of an omnidirectional antenna. Such a device could independently determine the direction and strength of an incident GW using just a single site, rather than requiring a network of GW detectors, as is the case with the currently operating interferometric detectors. A spherical antenna, first proposed in the 1970s by Forward [1] and Wagoner and Paik [2], would offer isotropic sensitivity, as a uniform sphere has five degenerate elastic quadrupole modes,

*Author to whom any correspondence should be addressed.

each maximally sensitive to a different polarization and direction of incoming GWs. Furthermore, for the same mass, the sphere would increase the interaction cross-section over the state-of-the-art cylindrical and bar detectors by a factor of about 5 [2]. The response of the sphere itself must ultimately be measured by one or more displacement sensors. An important development was the discovery by Johnson and Merkowitz [3, 4] of the truncated icosahedral pattern of sensors, more commonly known as TIGA. This arrangement has a valuable feature, namely, that it has isotropic sky coverage using six radial transducers on a single spherical antenna.

In the quest for a mid-frequency spherical antenna with high sensitivity, Paik *et al* proposed superconducting omnidirectional gravitational radiation observatory (SOGRO) [5, 6] in which, rather than a single sphere, there are six equal test masses (TMs) suspended from a common rigid platform in an octahedral configuration. SOGRO is another omnidirectional full-tensor GW detector. The six TMs must each sense all three translational modes. The SOGRO with a 50 m baseline would be sensitive enough to detect GWs from IMBH binaries and fill the missing frequency band 0.1–10 Hz between laser interferometer space antenna [7] and the planned third-generation ground-based detectors, cosmic explorer [8] and Einstein telescope [9]. Major challenges still lie ahead for SOGRO, as it requires large-scale cryogenics, advanced superconducting quantum interference devices (SQUIDs), and low-frequency three-axis suspension systems for its TMs.

Here, we propose a new TM configuration with the same features as SOGRO but requiring only four TMs as opposed to six. We show explicitly the combination of TM motions that can be used to give isotropic full-sky coverage, and reconstruct the full gravity gradient tensor. Hence, with only four properly aligned TMs, the incoming GW can be localized in the sky, modulo 180 degrees. Since weakly suspending TMs in the vertical direction is difficult due to the strong gravity bias, we also examine the case where only the horizontal motion of the four TMs is measured. The antenna patterns for these two cases are presented and compared to the currently operating interferometric detectors' antenna pattern.

2. TM configuration

We propose a new geometry using only four TMs to achieve full-tensor isotropic coverage. Figure 1 shows the locations of the accelerometers for the three patterns discussed here. Figure 1(a) presents the TIGA formation, which has isotropic sky coverage with six *radial* accelerometers. Paik and Venkateswara [10] discovered that six accelerometers *tangent* to the surface of the sphere also result in an isotropic sensitivity. Figure 1(b) presents the *octahedral* formation used in the proposed SOGRO design [5]. Finally, figure 1(c) presents the novel, *tetrahedral* formation, which has many of the same characteristics as the octahedral formation, using two fewer TMs. Since GWs (assuming general relativity) couple only to the five spheroidal quadrupole modes of the sphere, the six accelerometers in the TIGA and SOGRO configuration overdetermine the GW signals. The extra condition that the GW signals must satisfy provides a stronger rejection capability for non-GW events.

In this geometry, the TMs are positioned at the vertices of a regular tetrahedron, inscribed in a sphere of radius R. These four points can also be visualized as alternating vertices of a cube, and in figure 1(c) we have oriented the cube with its edges parallel to Cartesian coordinate axes. The positions of the four TMs, M_i, are then given by

$$M_1 : \frac{R}{\sqrt{3}}(1,1,1), \quad M_2 : \frac{R}{\sqrt{3}}(-1,1,-1), \quad M_3 : \frac{R}{\sqrt{3}}(1,-1,-1), \quad M_4 : \frac{R}{\sqrt{3}}(-1,-1,1). \tag{1}$$

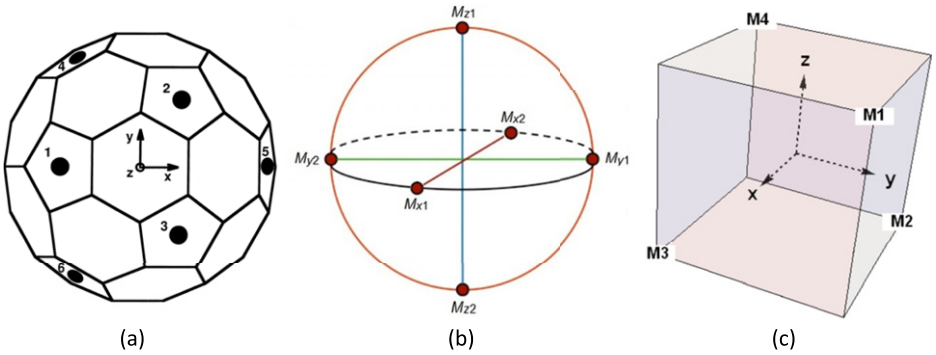

Figure 1. Accelerometer configuration options for forming a full-tensor GW detector. (a) Icosahedral configuration of six accelerometers on a hemisphere Reprinted figure with permission from [4], Copyright (1995) by the American Physical Society., (b) octahedral configuration of six accelerometers on the entire sphere, and (c) tetrahedral configuration of four accelerometers on four of the eight vertices of a cube.

We can relate each element of the GW strain tensor to the displacements of the TMs using

$$x_{ij} = \sum_{k=1}^{3} \frac{h_{jk} u_{ik}}{2}, \quad i, j = 1, 2, 3 \tag{2}$$

where x_{ij} is the displacement of the ith TM in the j direction, h_{jk} are the GW strain tensor components, and u_{ik} is the kth coordinate of the position of the ith TM. The motion of these TMs can be combined to reconstruct each element of h_{ij} using a procedure similar to that outlined in Paik *et al* [5] for SOGRO:

$$h_{ii} = \frac{2}{L}\left(x_{ii+} - x_{ii-}\right) \tag{3}$$

$$h_{ij} = \frac{1}{L}\left(\left(x_{ij+} - x_{ij-}\right) + \left(x_{ji+} - x_{ji-}\right)\right) \; i \neq j \tag{4}$$

where $L = 2R$ is the baseline of the SOGRO detector, and x_{ij+} represents the motion in the i direction for a TM lying on the positive j axis, with the sign $i/j+$ and $i/j-$ indicating whether the TM is positioned at $+L$ or $-L$ along the i/j-axis. Therefore, we difference the displacements of two TMs separated along the coordinate axis in question to measure the differential-mode (DM) signal. For example, in the case of SOGRO, h_{xx} is the DM displacement between the TMs located on the positive and negative x axis.

In the coordinate system we use for the tetrahedral configuration, however, none of the TMs lie on the coordinate axes. In this case, we must first combine the common-mode (CM) displacement between the two TMs with positive x values, TMs 1 and 3, and the CM displacement between the two TMs with negative x coordinates, TMs 2 and 4. Then we take the difference between the two CM signals in order to produce h_{xx}. Note that in the tetrahedral case, the effective arm-length between TMs, $L = \frac{2R}{\sqrt{3}}$. The following expressions are found for each element of the GW tensor:

$$h_{xx} = \frac{\sqrt{3}}{R}\left(\frac{x_{1x} + x_{3x}}{2} - \frac{x_{2x} + x_{4x}}{2}\right) \tag{5a}$$

$$h_{yy} = \frac{\sqrt{3}}{R}\left(\frac{x_{1y}+x_{2y}}{2} - \frac{x_{3y}+x_{4y}}{2}\right) \tag{5b}$$

$$h_{zz} = \frac{\sqrt{3}}{R}\left(\frac{x_{1z}+x_{4z}}{2} - \frac{x_{2z}+x_{3z}}{2}\right) \tag{5c}$$

$$h_{xy} = \frac{\sqrt{3}}{2R}\left(\left(\frac{x_{1y}+x_{3y}}{2} - \frac{x_{2y}+x_{4y}}{2}\right) + \left(\frac{x_{1x}+x_{2x}}{2} - \frac{x_{3x}+x_{4x}}{2}\right)\right) \tag{5d}$$

$$h_{xz} = \frac{\sqrt{3}}{2R}\left(\left(\frac{x_{1z}+x_{3z}}{2} - \frac{x_{2z}+x_{4z}}{2}\right) + \left(\frac{x_{1x}+x_{4x}}{2} - \frac{x_{2x}+x_{3x}}{2}\right)\right) \tag{5e}$$

$$h_{yz} = \frac{\sqrt{3}}{2R}\left(\left(\frac{x_{1z}+x_{2z}}{2} - \frac{x_{3z}+x_{4z}}{2}\right) + \left(\frac{x_{1y}+x_{4y}}{2} - \frac{x_{2y}+x_{3y}}{2}\right)\right). \tag{5f}$$

In the tetrahedral case there are four TMs, each measuring three displacement components, giving 12 measurement channels in total. These can be combined to produce 12 signal channels, corresponding to three CM displacements, three CM rotations, the five components of the GW tensor, and finally one Laplace-equation violating radial (monopole) 'breathing mode', which acts as a null channel for general relativity. This final channel can be used to search for a scalar wave predicted by some alternative theories, such as the Brans–Dicke theory [12].

In the ideal case, by combining the signals this way, we reject the CM in order to isolate the DM response due to the GW. In practice sufficient CM rejection is difficult to achieve. For the case of a set of accelerometers mounted on a common, rigid platform, the signals are combined at the input of a DC SQUID prior to amplification and digitization, and small differences in response and calibration of these sensors could lead to the gravity gradient signals being swamped by imperfectly subtracted seismic noise. Therefore, precise CM balancing of this instrument is essential in order to reach the intrinsic sensitivity of the detector [5]. Misalignment of the sensor would also lead to off-axis accelerations coupling into the gradiometer output, and so the instrument requires either precise mechanical tolerances, or some mechanism of adjusting the axis alignment *in situ*.

3. Omnidirectionality of tetrahedral configuration

We determine the omnidirectionality by looking at the response of the four TMs to a plane wave GW propagating in a radial direction with polar angle θ, azimuthal angle φ, and polarization angle ψ. In this coordinate system, each of the angles being zero corresponds to a GW propagating from the positive z axis with + polarization in the lab frame. Then, using equation (2), we sum the squares of the displacement of each accelerometer due to this $h_{jk}(\theta, \varphi, \psi)$ to get the power of the response.

In figure 2(a), we show the polarization-averaged response of the tetrahedron to a GW incident from (θ, φ). Figure 2(b) shows the directional dependence of an L-shaped interferometer detector such as LIGO [11] for comparison. Unlike the laser interferometer-based detectors, this tetrahedral formation provides *isotropic* full-sky coverage to GWs, similar to SOGRO and TIGA. For this calculation, the LIGO-like detector's arms are diagonal to the x and y axes (rotated $\pi/4$ around the z axis), so the antenna pattern is $1/4$ of its own maximum at ($\theta = \pi/2$, $\varphi = \pi/4$) and is 0 along the x and y axes. The maximum polarization-averaged response for the LIGO-like detector is $1/2$ that of the tetrahedron because the LIGO-like detector is only

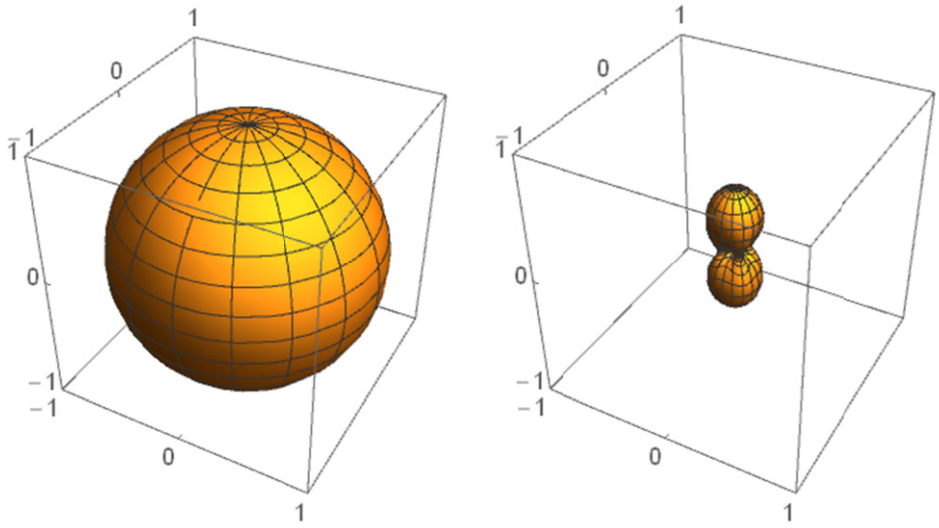

Figure 2. Polarization-averaged antenna patterns of (a) tetrahedron vs (b) LIGO. The antenna pattern for the tetrahedron is perfectly spherical, representing isotropic sky coverage, while the antenna pattern for a LIGO-like detector is at a maximum along the z axis. The maximum polarization-averaged response for the LIGO-like detector is $1/2$ that of the tetrahedron because the LIGO-like detector is only sensitive to the $\times$ polarization along the z axis, while the tetrahedral arrangement is equally sensitive to both the + and $\times$ polarizations.

sensitive to the $\times$ polarization along the z axis, while the tetrahedral arrangement is equally sensitive to both the + and $\times$ polarizations. A detailed discussion of how the plots in figure 2 are produced can be found in the appendix.

For *co-located* LIGO-like detectors, at least four detectors with different orientations would be necessary to determine the direction and polarization of the most general GW signal. However, a network of interferometric detectors at different locations on the Earth, such as LIGO + Virgo + KAGRA, record the passing GW signal at different times as well as with different detector orientations. The time delay between detectors is typically comparable to the period of signals in the sensitive band, which allows triangulation to be used to better localize sources and break degeneracies, see for instance [13]. Also, for modeled astrophysical signals such as binary inspirals, relations between the polarization components allow sources to be located with fewer detectors. The reconstruction accuracy of the network is however highly anisotropic.

4. Lab-frame horizontal modes only

One challenge for the implementation of this design, as mentioned in section 1, is that weakly suspending a TM in all three directions is difficult due to the gravity bias. It is of interest to analyze what the directional sensitivity plot looks like if only horizontal displacements are measured. Such a system is simpler to implement and could consist only of pendulum systems or magnetically levitated TMs. Therefore, in this section, we simply set $x_{iz} = 0$ in equations (5a)–(5f), to produce equations (6a)–(6e) for the GW tensor components.

However, the absence of vertical components of acceleration would not allow a direct measurement of h_{zz}. If we assume general relativity, h_{zz} could be obtained from the tracelessness condition of the GW tensor, as in equation (6f). This condition is in turn a result of the gravitational potential in a vacuum obeying Laplace's equation. In doing this, we would be sacrificing the possibility of detecting a scalar wave predicted by some alternative theories [12]. The equations for h_{ij} in the case of measuring only horizontal displacements are found to be

$$h_{xx} = \frac{\sqrt{3}}{R}\left(\frac{x_{1x} + x_{3x}}{2} - \frac{x_{2x} + x_{4x}}{2}\right) \tag{6a}$$

$$h_{yy} = \frac{\sqrt{3}}{R}\left(\frac{x_{1y} + x_{2y}}{2} - \frac{x_{3y} + x_{4y}}{2}\right) \tag{6b}$$

$$h_{xy} = \frac{\sqrt{3}}{2R}\left(\left(\frac{x_{1y} + x_{3y}}{2} - \frac{x_{2y} + x_{4y}}{2}\right) + \left(\frac{x_{1x} + x_{2x}}{2} - \frac{x_{3x} + x_{4x}}{2}\right)\right) \tag{6c}$$

$$h_{xz} = \frac{\sqrt{3}}{R}\left(\frac{x_{1x} + x_{4x}}{2} - \frac{x_{2x} + x_{3x}}{2}\right) \tag{6d}$$

$$h_{yz} = \frac{\sqrt{3}}{R}\left(\frac{x_{1y} + x_{4y}}{2} - \frac{x_{2y} + x_{3y}}{2}\right) \tag{6e}$$

$$h_{zz} = -(h_{xx} + h_{yy}). \tag{6f}$$

The difference between equations (6d) and (5e) can be understood as follows. The amplitude of the DM signal of the vertically separated CM motion in the x direction should be the same amplitude as the unmeasured DM signal of the x-separated CM motion in the z direction as long as there is sufficient rotational isolation from seismic noise. Therefore, we can still recover h_{xz} (and by a similar approach, h_{yz}) by doubling the amplitude of the signal in the measured arm. This is a similar step to that done in Paik *et al* for SOGRO [6].

This can also be seen by comparing the measured degrees of freedom with the three-axis case. We now only have 8 rather than 12 measurement channels. From this, we construct eight signal channels, corresponding to two CM displacements (x and y), three CM rotations (about the x, y and z-axis), three pure (assuming there is no signal in the radial breathing mode) components of the GW tensor (h_{xx}, h_{yy} and h_{xy}). In addition, the last two tensor components (h_{xz} and h_{yz}) can be recovered from two CM rotations (about the x and y axes) since the pendulum suspension ensures that there should be negligible CM rotation signal in the tilt modes.

The antenna pattern for the polarization-averaged response is shown in figure 3. This detection scheme is clearly no longer isotropic. However, it maintains sensitivity in all regions of the sky. The ratio of the maximum sensitivity to minimum is 2:1 in power. It is worth noting also that this is the same ratio as six horizontal TMs in the SOGRO arrangement. Therefore, this tetrahedral arrangement can achieve the same direction-dependent sensitivity as SOGRO with the appropriate baseline and TMs.

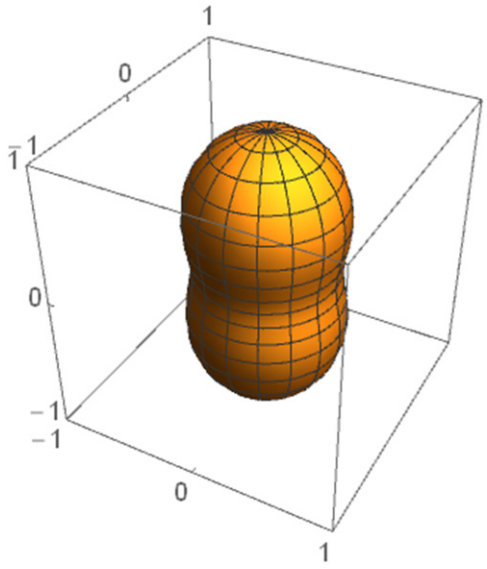

Figure 3. Antenna pattern for the tetrahedral configuration using only the horizontal motion of each TM. The maximum value for this antenna pattern is along the z axis and is the same value as the spherical case. However, in the xy plane, the value dips to a minimum that is $1/2$ of the maximum value.

5. Conclusion

We have shown that four three-axis superconducting accelerometers arranged in a tetrahedron provide isotropic, full-sky coverage for the entire GW tensor. Additionally, this arrangement of four three-axis sensors provides full-sky coverage and allows the incoming signal to be reconstructed modulo 180 degrees. In order to reach the detector noise of each sensor, the analog acceleration signals from all four accelerometers must be combined in precise proportions before they are amplified by a DC SQUID. This requires accurate alignment of the sensors and fine adjustments of the calibration of the readout circuits.

Since it is difficult to weakly suspend TMs and thus achieve high acceleration sensitivity in the vertical direction, we also considered the possibility of using only horizontal measurements of the TMs. However, sacrificing the vertical motion of the TMs removes the omnidirectionality and the ability to directly measure h_{zz}. Nevertheless, we achieve the same antenna pattern as SOGRO in both the three-axis and horizontal sensor cases.

Acknowledgments

We acknowledge useful discussions with Vol Moody and Ronald Norton. This work was partly supported by NASA Grant 80NSSC19K0447 and NSF Grant PHY1912627.

Data availability statement

No new data were created or analysed in this study.

Appendix. Derivation of antenna pattern

Here, we will show the steps to deriving an antenna pattern for a set of three-axis accelerometers to an incoming GW. We begin with a $+$-polarized GW incident along the positive z-axis:

$$h_0 = \begin{pmatrix} h & 0 & 0 \\ 0 & -h & 0 \\ 0 & 0 & 0 \end{pmatrix} \tag{7}$$

where h is a unitless measure of the strength of the GW. Then, we give the GW a polarization, ψ, by rotating h_0 about the z axis:

$$h_{\mathrm{pol}}(\psi) = \begin{pmatrix} \cos(\psi) & -\sin(\psi) & 0 \\ \sin(\psi) & \cos(\psi) & 0 \\ 0 & 0 & 1 \end{pmatrix} h_0 \begin{pmatrix} \cos(\psi) & \sin(\psi) & 0 \\ -\sin(\psi) & \cos(\psi) & 0 \\ 0 & 0 & 1 \end{pmatrix}. \tag{8}$$

Next, we allow the GW to come from any point in the sky, defined by (θ, φ), by rotating about the y axis by θ and then about the z axis by φ:

$$\begin{aligned} h_{\mathrm{rot}}(\theta, \varphi, \psi) = &\begin{pmatrix} \cos(\varphi) & -\sin(\varphi) & 0 \\ \sin(\varphi) & \cos(\varphi) & 0 \\ 0 & 0 & 1 \end{pmatrix} \begin{pmatrix} \cos(\theta) & 0 & \sin(\theta) \\ 0 & 1 & 0 \\ -\sin(\theta) & 0 & \cos(\theta) \end{pmatrix} h_{\mathrm{pol}}(\psi) \\ &\times \begin{pmatrix} \cos(\theta) & 0 & -\sin(\theta) \\ 0 & 1 & 0 \\ \sin(\theta) & 0 & \cos(\theta) \end{pmatrix} \begin{pmatrix} \cos(\varphi) & \sin(\varphi) & 0 \\ -\sin(\varphi) & \cos(\varphi) & 0 \\ 0 & 0 & 1 \end{pmatrix}. \end{aligned} \tag{9}$$

We next define the positions, u_i, of the three-axis accelerometers, relative to their collective center of figure:

$$\overrightarrow{u_i} = \begin{pmatrix} u_{ix} \\ u_{iy} \\ u_{iz} \end{pmatrix} = u_{ik} \tag{10}$$

where i indexes the accelerometers and $k = x, y, z$ indexes the component of the position. The displacement induced on each TM by the GW is given by

$$\overrightarrow{x_i}(\theta, \varphi, \psi) = \frac{h_{\mathrm{rot}}(\theta, \varphi, \psi)\overrightarrow{u_i}}{2}. \tag{11}$$

Note that equation (11) is the same as equation (2), except that here we have explicitly written the dependence on θ, φ, and ψ and used the matrix and vector notation as opposed to the i and j subscripts.

Finally, we calculate the polarization-averaged sensitivity of the detector by summing in quadrature the displacements of each TM, giving the following expression:

$$\overline{R}(\theta, \varphi) = \frac{1}{\pi}\int_0^{\pi} \mathrm{d}\psi \sum\nolimits_i \|\overrightarrow{x_i}(\theta, \varphi, \psi)\|^2. \tag{12}$$

This $\overline{R}(\theta, \varphi)$ is what we have shown in figures 2 and 3. The only difference when taking only the horizontal motion of the accelerometers is that in equation (12), we set the z component of $\overrightarrow{x_i}(\theta, \varphi, \psi)$ to zero. Furthermore, in the discussion of figures 2 and 3, we set the maximum

value of $\overline{R}(\theta, \varphi)$ to 1 if the antenna is equally sensitive to both GW polarizations by adjusting h in equation (7) accordingly.

ORCID iDs

Zachary Metzler https://orcid.org/0000-0002-1236-8510
Ho Jung Paik https://orcid.org/0000-0001-8303-4529
Peter S Shawhan https://orcid.org/0000-0002-8249-8070

References

[1] Forward R L 1971 Multidirectional, multipolarization antennas for scalar and tensor gravitational radiation *Gen. Relativ. Gravit.* **2** 149
[2] Wagoner R V and Paik H J 1977 Multi-mode detection of gravitational waves by a sphere *Proc. Int. Symp. Experimental Gravitation* pp 257–65
[3] Johnson W W and Merkowitz S M 1993 Truncated icosahedral gravitational wave antenna *Phys. Rev. Lett.* **70** 2367
[4] Merkowitz S M and Johnson W W 1995 Spherical gravitational wave antennas and the truncated icosahedral arrangement *Phys. Rev.* D **51** 2546
[5] Paik H J, Griggs C E, Moody M V, Venkateswara K, Lee H M, Nielsen A B, Majorana E and Harms J 2016 Low-frequency terrestrial tensor gravitational-wave detector *Class. Quantum Grav.* **33** 075003
[6] Paik H J, Moody M V and Norton R S 2020 SOGRO—terrestrial full-tensor detector for mid-frequency gravitational waves *Int. J. Mod. Phys.* D **29** 1940001
[7] Amaro-Seoane P *et al* 2012 Low-frequency gravitational-wave science with eLISA/NGO *Class. Quantum Grav.* **29** 124016
[8] Evans M *et al* 2021 A horizon study for cosmic explorer: science, observatories, and community *Cosmic Explorer Technical Report*
[9] Hild S *et al* 2011 Sensitivity studies for third-generation gravitational wave observatories *Class. Quantum Grav.* **28** 094013
[10] Paik H J and Venkateswara K Y 2009 Gravitational wave detection on the Moon and the moons of Mars *Adv. Space Res.* **43** 167
[11] Abbott B P *et al* 2009 LIGO: the laser interferometer gravitational-wave observatory *Rep. Prog. Phys.* **72** 076901
[12] Brans C H and Dicke R H 1961 Mach's principle and a relativistic theory of gravitation *Phys. Rev.* **124** 925
[13] Essick R, Vitale S, Katsavounidis E, Vedovato G and Klimenko S 2015 Localization of short duration gravitational-wave transients with the early advanced LIGO and Virgo detectors *Astrophys. J.* **800** 81